

^1H NMR investigation of the magnetic spin configuration in the molecule-based ferrimagnet $[\text{MnTFPP}][\text{TCNE}]$

M. Fardis,* G. Diamantopoulos, and G. Papavassiliou

Institute of Materials Science, National Center for Scientific Research "Demokritos," 15310 Athens, Greece

K. Pokhodnya

*Department of Chemistry, 315 South 1400 East, University of Utah, Salt Lake City, Utah 84112-0850
and Department of Chemistry, The Ohio State University, Columbus, Ohio 43210*

Joel S. Miller and D. K. Rittenberg

Department of Chemistry, 315 South 1400 East, University of Utah, Salt Lake City, Utah 84112-0850

C. Christides

Department of Engineering Sciences, School of Engineering, University of Patras, 26500 Patras, Greece

(Received 30 August 2001; revised manuscript received 5 April 2002; published 16 August 2002)

^1H NMR line-shape measurements have been performed in the linear chain molecule-based ferrimagnet $[\text{MnTFPP}][\text{TCNE}] \cdot x\text{PhMe}$ (TFPP=tetrakis(4-fluorophenyl)porphinato; TCNE=tetracyanoethylene) as a function of temperature. Hyperfine shifts of opposite sign were observed indicating the presence of two oppositely hyperfine couplings, predominantly between the Mn ions and the ^1H nuclei of the planar ring of the $[\text{MnTFPP}]^+$ unit. The observation of the hyperfine shifts strongly suggests the existence of two oppositely directed $[\text{MnTFPP}]^+$ sites. Since there is no direct exchange coupling between adjacent $[\text{MnTFPP}]$ spins, then it can be argued that an ordered spin configuration with antiparallel components may arise from antisymmetric spin-spin exchange interactions. The field independence of the hyperfine shifts at low temperatures and for applied magnetic fields in the range 2–5 T, indicates the presence of ferromagnetic interactions in the ground state of the ferrimagnetic chain.

DOI: 10.1103/PhysRevB.66.064422

PACS number(s): 75.50.Xx, 76.60.-k, 33.25.+k

I. INTRODUCTION

Molecule-based magnets have been intensively investigated since the discovery^{1,2} in the 1980s of molecule-based materials exhibiting a spontaneous magnetization below a critical temperature T_c . Much attention is paid to the origin of the magnetic ground state, the function-structural relation, and the design of new high- T_c molecular magnets.³ In addition, the spin alternating, chainlike structure of most of those materials, makes them ideal for the study of the magnetic behavior of low-dimensional magnets with mixed quantum/classical spin systems.^{4–6}

$[\text{MnTFPP}][\text{TCNE}]$ (TFPP=tetrakis(4-fluorophenyl) porphinato; TCNE=tetracyanoethylene) is a substituted electron transfer salt belonging to the manganeseporphyrin family⁷ $[\text{Mn}^{\text{III}}\text{TPP}][\text{TCNE}] \cdot x\text{solvent}$ (TPP=meso-tetraphenylporphyrinato). This class of materials comprises chains of alternating $S=2$ metalloporphyrin cations and $S=1/2$ cyanocarbon anions (e.g., Fig. 1). Planar $[\text{TCNE}]^-$ lies between the planes of $[\text{MnTXPP}]^+$ and directly coordinates to two Mn^{III} leading to strong antiferromagnetic exchange ($J \leq 100$ K for $H = -2J\mathbf{S}_a \cdot \mathbf{S}_b$) along the chains. The chains are separated by the solvent molecules. In an effort to establish structure-function relationships, a series of substituted manganese tetraphenylporphyrin TCNE electron transfer salts $[\text{MnTXPP}][\text{TCNE}]$ ($X = \text{F}, \text{Cl}, \text{Br}, \text{I}$) have been recently^{8,9} investigated. The high-temperature behavior of these systems is consistent

with one-dimensional (1D) ferrimagnetic character whereas at low temperatures ($T < 50$ K) the systems exhibit unusual magnetic properties similar to those encountered in glassy/disordered or superparamagnetic spin systems. Particularly for $[\text{MnTFPP}][\text{TCNE}] \cdot x\text{PhMe}$, the magnetic susceptibility data $\chi(T)T$ were analyzed according to the Seiden model⁶ for antiparallel coupled, alternating classical, and quantum spin sites yielding an intrachain coupling constant^{8,10} $J_{\text{intra}} = -225$ K. At 2 K the 9 T magnetization approaches $(3/2)\mu_B$ per $[\text{MnTFPP}][\text{TCNE}]$ formula unit, which should be expected for the Mn^{III} $S=2$ antiferromagnetically coupled to $[\text{TCNE}] S=1/2$. The system undergoes a magnetic transition at $T_c = 28$ K (with peaks in the real and imaginary parts of the ac-susceptibility).⁸ This value is the highest for the family of porphyrin-based magnets synthesized so far. However, below 10 K the system freezes into a cluster spin-glass-like state with a small remanence, relatively low coercive field and paramagnetic-like magnetization field dependence below a certain threshold field. Below 5 K metamagnetic-like behavior is observed with increasing coercive fields that approach $H_{cr} = 21.8$ KOe at 2 K.^{8,9} Above this field the magnetization rises rapidly, indicating a significant rearrangement of spins. The nature of this state remains unclear.

Despite the large amount of experimental data, demonstrating frequency-dependent ac-susceptibility, irreversibility in the magnetization, field dependence of the bifurcation

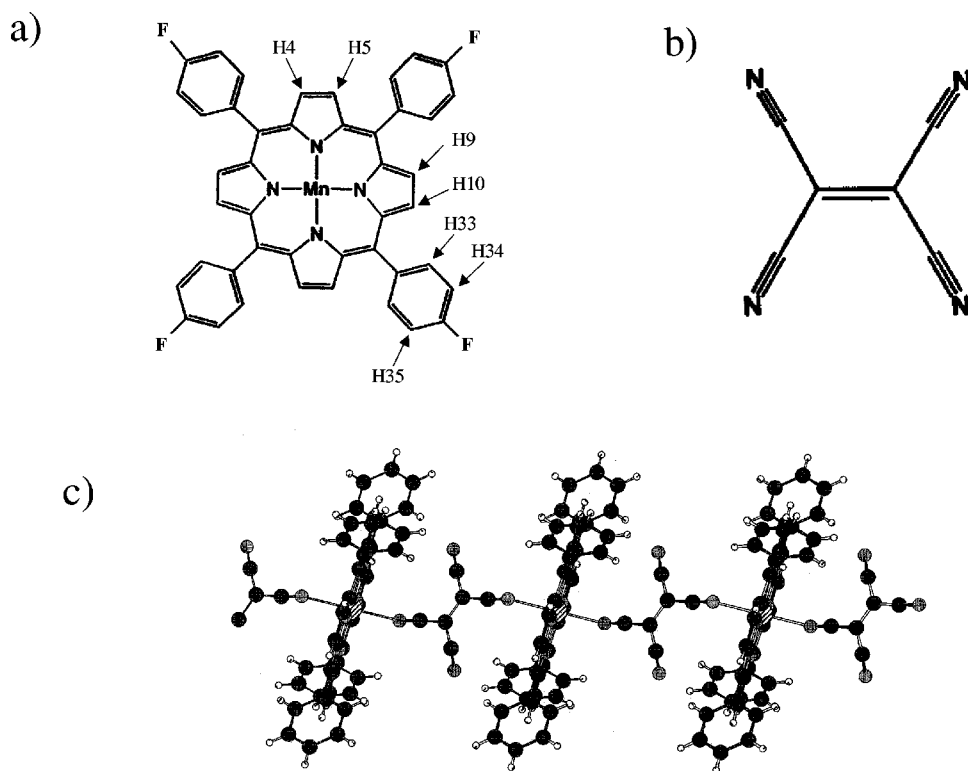


FIG. 1. (a) $[\text{MnTFPP}]^+$, (b) $[\text{TCNE}]^-$, and (c) structure of the $[\text{MnTFPP}][\text{TCNE}]$ molecular chain.

point in the field-cooled (FC) and zero-field-cooled (ZFC) magnetizations, hysteresis effects, the nature of the magnetically ordered ground state in these 1D systems is not yet well understood.^{9,11–14} The observed metamagnetic-like behavior at low temperatures ($T < 5$ K) in these substituted manganese porphyrin electron transfer salts has been recently ascribed to a field induced state of canted antiferromagnetism.⁹

In this study we report the results of ^1H NMR line-shape measurements in the linear chain ferrimagnet $[\text{MnTFPP}][\text{TCNE}] \cdot x\text{PhMe}$ as a function of temperature. Our aim is to probe locally the magnetic properties via the internal magnetic fields present in the molecular solid and therefore to acquire microscopic information for this class of materials.

II. EXPERIMENTAL DETAILS

Two powder samples of $[\text{MnTFPP}][\text{TCNE}] \cdot x\text{PhMe}$ differing in the amount of solvent PhMe were investigated. The synthesis of the samples is described elsewhere.⁸ In the standard preparation of $[\text{MnTFPP}][\text{TCNE}] \cdot x\text{PhMe}$, solutions of $\text{MnTFPP}(\text{py})$ ($\text{py} = \text{pyridine}$) and TCNE dissolved in toluene are mixed and the product is collected by vacuum filtration, under oxygen- and water-free conditions. In the present work, one sample was dried under vacuum (resulting in partial dissolution), whereas the other sample was not.

^1H pulsed NMR experiments were performed at 2.35 and 4.7 T using a home-built and a Bruker MSL 200 spectrometer, operating at 100.113 and 200.145 MHz, respectively. Two Oxford 1200CF continuous flow cryostats were employed for measurements in the range 4–300 K. ^1H line-shapes measurements were performed at both fields. At high temperatures, where a single pulse of $\sim 1.5\text{--}4$ μs was suf-

ficiently strong to irradiate the whole NMR line, the spectrum was obtained by the Fourier transform of the nuclear free induction decay at the Larmor frequency. For low-temperature measurements, the spectrum was obtained by the spin-echo point-by-point method while varying the frequency, because of the large width of the resonance line. Magnetic measurements were performed in a Quantum Design MPMSR2 superconducting quantum interference device magnetometer.

III. RESULTS AND DISCUSSION

Thermomagnetic curves (Fig. 2) have been measured at 100 G, 1 kG, and 48 kG. The samples were cooled in zero field, then the field was applied and the data were collected

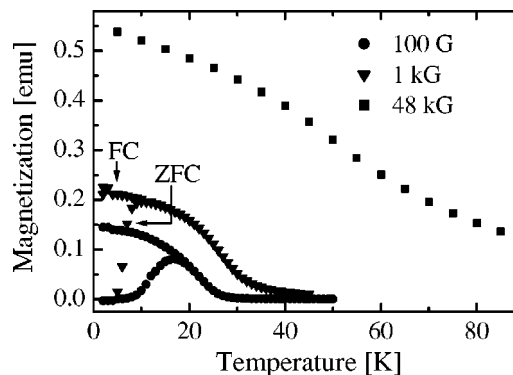


FIG. 2. Temperature dependence of the bulk magnetization for various magnetic fields. The field-cooled and zero-field-cooled branches of the magnetization are indicated as (FC) and (ZFC), respectively.

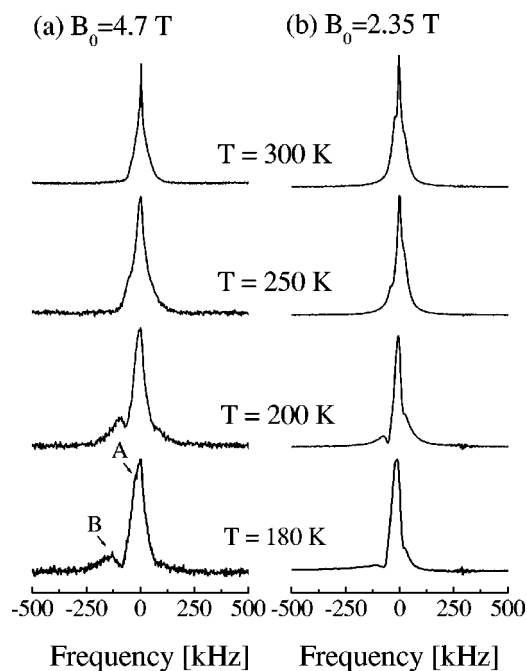


FIG. 3. ^1H NMR spectra at (a) $B_0=4.7$ T and (b) $B_0=2.35$ T for selected high temperatures.

while warming (ZFC) and subsequent cooling (FC). The two different samples gave identical results. The low-field data indicate the presence of a field-dependent bifurcation point in accordance with previous studies.^{8,11} Such magnetic history-dependent effects are characteristic for systems with a frozen-in spin disordered state. The shift of the bifurcation point with the applied field is a direct evidence that the number of multiple minima on the free-energy surface decreases as the external field increases.¹⁵ The origin of frustration and disorder, which are both necessary for a proper explanation of the low-temperature behavior, is, however, not yet known. As will be shown below, the NMR spectra reveal two magnetically nonequivalent Mn sites with opposite sign of magnetization, indicating the establishment of competing interactions at low temperatures.

^1H NMR line-shape measurements were performed as a function of temperature. NMR provides important information in magnetic materials through the local field at the nucleus produced by the magnetic ions. The main interaction in these NMR experiments is that between the proton nuclei and the electrons, so the nuclei can be considered as local probes for the static and dynamical electronic spin correlations. Typical ^1H NMR spectra at high temperatures at $B_0 = 4.7$ and 2.35 T are presented in Figs. 3(a,b), respectively. The high-temperature spectra are characterized by two lines which are progressively resolved as the temperature is lowered. This feature is similar for both fields. The central line [denoted as A in Fig. 3] does not shift appreciably with temperature, whereas the second line B shifts gradually on cooling towards lower frequencies. At these high temperatures the shift of the line B is in the kilohertz range and below 100 K increases to the megahertz range. The spectra at low temperatures are presented in Figs. 4 and 5 for $B_0=4.7$ and 2.35 T, respectively. The spectra at low temperatures are charac-

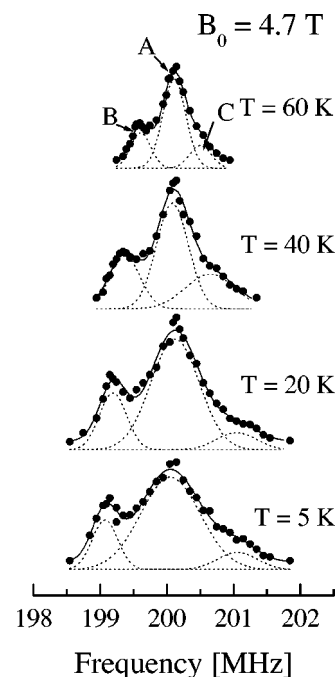


FIG. 4. ^1H NMR spectra at $B_0=4.7$ T for selected low temperatures. The dotted lines are Gaussian fits to the spectra.

terized also by a third line C displaced at higher frequencies. The low-temperature structure of the spectra is found similar for both applied fields. The two samples investigated gave identical results.

NMR shifts were determined from the position of the maxima of each spectrum with respect to the B_0/γ value. The maxima at low temperatures were obtained from a three-Gaussian line fit to the spectra (dotted lines in Figs. 4 and 5). The shift of the NMR line is determined by the total magnetic local fields acting on the nuclear sites, which in general is the sum of the hyperfine and the dipolar field.¹⁶ The frequency shifts $\Delta f^{(4.7)}$ and $\Delta f^{(2.35)}$ of the spectrum lines A, B, and C for $[\text{MnTFPP}][\text{TCNE}]$ for the whole temperature range are shown in Fig. 6 for the two applied magnetic fields.

The observed NMR shifts were not corrected for the effect of the demagnetization field. The demagnetization field shift arises from the finite volume magnetization of the sample, and hence the magnetic field inside the sample can be different from the applied field.¹⁶ Therefore, demagnetization effects are most significant for large magnetizations, i.e., for samples with large bulk susceptibilities in large applied magnetic fields. For a spherical particle, demagnetization and Lorentz fields cancel, so that one need not correct the measured NMR shifts for these fields. It is difficult to say whether or not these fields contribute slightly to the field shift measured in a powder of arbitrary shaped particles. In our sample in the high-temperature quasi-paramagnetic phase, the demagnetization field will certainly be negligible due to the small value of the bulk susceptibility. At low temperatures there is the possibility of the presence of a demagnetization field due to the large value of the magnetization. However, in view of the fact that the absolute value of the NMR shift is the same for $B_0=4.7$ and 2.35 T in this temperature regime (Fig. 6), it may be argued that the demagne-

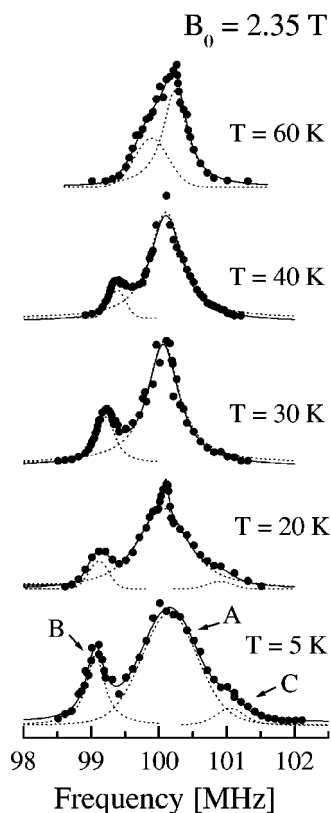


FIG. 5. ^1H NMR spectra at $B_0=2.35$ T for selected low temperatures. The dotted lines are Gaussian fits to the spectra.

tization field correction is smaller than the error associated with the determination of the NMR shift. Also, the demagnetization field exactly cancels out when one considers the differences in the shifts between the central peak A and the peaks B and C.

In an effort to assign the observed spectra lines to proton groups in the compound's formula unit, reference is made to the schematic structure of $[\text{MnTFPP}]^+$ porphyrin unit in Fig. 1(a), labeling the proton sites $H4, H5, H9, H10, \dots$ of the planar ring and the proton sites $H33, H34, H35, \dots$ of the phenyl ring.¹⁷ The first group of the eight pyrrole protons $H4, H5, H9, H10, \dots$ are the nearest neighbors to the Mn^{III} ion with a distance of ~ 5.1 Å therefore are considered as magnetically equivalent. The second group of 16 protons $H33, \dots, H35, \dots$ is at relatively larger distances than the pyrrole protons. There is also a third group of protons, those of the solvate, which intercalate between the planar rings and the chains of the molecular solid which are not shown in Fig. 1.

An order of magnitude calculation of the dipolar interaction considering the distances of the protons involved, indicates that the dipolar shifts are mainly in the kilohertz region in the Mn^{III} porphyrin compounds. The small shifts of the spectrum line A are thus consistent with the dipolar interaction. Thus, the central line A originates from protons that are coupled to Mn moments via dipolar interactions only, which yield a broadening of the line and a small shift. These protons are the phenyl and the solvate protons. The large and equal-in-magnitude shifts of lines B and C are tentatively

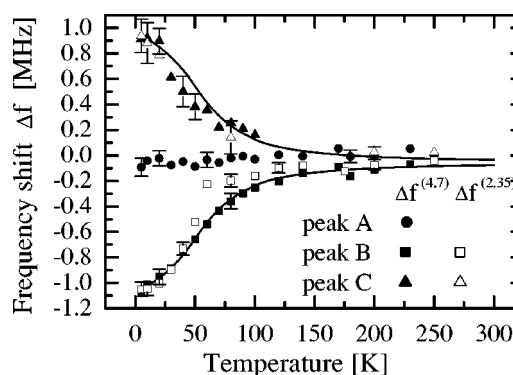


FIG. 6. Temperature dependence of the frequency shift $\Delta f^{(4.7)}$ and $\Delta f^{(2.35)}$ of the three peaks in the ^1H NMR spectra. The solid lines demonstrate the scaling of the NMR shift with the bulk magnetization as described in the text.

ascribed with the pyrrole protons of the planar ring and experience a transferred hyperfine field due to the delocalized spin density¹⁸ on the Mn^{III} ion. This is consistent with previous NMR studies of a series of Mn^{III} porphyrin solution complexes.^{19,20} These studies have demonstrated that the minimal magnetic anisotropy and small zero-field splitting of a porphyrin coordinated Mn^{III} ion ensure that the isotropic shifts of the pyrrole protons (lines B and C) arise almost entirely from “through bond” Fermi contact interactions.

Since the NMR shift is related to the average magnetic field at the proton site, it directly probes the (average) macroscopic susceptibility according to the relation $K = (A/\gamma_N\gamma_e\hbar^2)\chi$, where K is the fractional shift, A is the isotropic hyperfine coupling constant, γ_N and γ_e are the gyromagnetic ratios of the proton and electron, respectively, and χ is the static susceptibility.²¹ This relation is nicely demonstrated in Fig. 7, in the so-called $K-\chi$ plot,²¹ where the shift $K^{(4.7)}$ for the line B is plotted as a function of the susceptibility²² at the applied field $B_0=4.7$ T, with the temperature as an implicit parameter. Within the errors, all the experimental points fit a straight line. The fits for both spectrum lines B and C give $K^{(4.7)} = \mp 0.93\chi - 0.028\%$, where χ

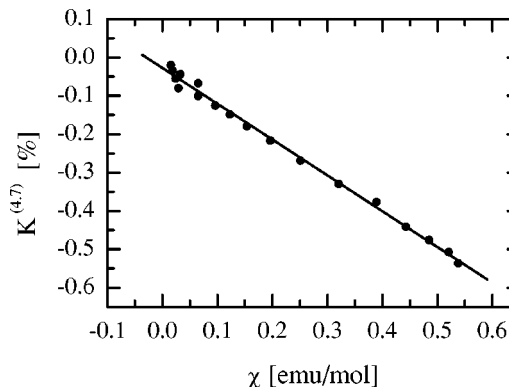


FIG. 7. Fractional NMR shift $K^{(4.7)}$ as a function of the static susceptibility χ for the peak B with temperature as an implicit parameter. The solid line is a linear fit to the data as described in the text.

is in emu/mol while the constant term can be related with the small dipolar contribution and the paramagnetic impurities in the magnetization data. From the fit, one finds $A = -1.5 \times 10^{-5} \text{ cm}^{-1}$. It is pointed out that the linear relation between K and χ holds for the whole temperature range investigated (5–300 K). This indicates that by measuring the temperature dependence of the local fields at the proton sites, we can, in principle, study the temperature variation of the component of the magnetization in the direction of the external field.

The frequency shift at 4.7 T as a function of temperature according to the above fit is also plotted as solid lines in Fig. 6. It is thus established that the frequency shift of the NMR spectrum follows the temperature dependence of the static susceptibility over the entire temperature range investigated. The shifts of the spectrum lines B and C are of almost the same magnitude, but with opposite signs within the experimental error particularly for spectrum line C where the line is not well resolved (Figs. 4 and 5). Since lines B and C were ascribed to the same group (equivalent pyrrole protons), the opposite sign means that there are Mn^{III} ions with opposite magnetic components along the direction of the external field.

The presence of two nonequivalent Mn magnetic sites in $[\text{MnTPP}][\text{TCNE}]$ compounds is an important information for this family of compounds. The structure consists of chains of manganeseporphyrins linked by TCNE radicals, typically with only one crystallography unique Mn site. The shortest intrachain Mn-Mn distance is more than 10 Å and the interchain Mn-Mn distances are about 14.5 Å, therefore, only weak dipole-dipole interactions between Mn spins (but not an antiferromagnetic one) are apparently relevant.²³

The observation of two Mn sites with opposite spins is consistent with the observed metamagnetism in this family of materials.⁹ It has been argued⁹ that the observed S-shaped curves of the magnetization isotherms $M(H)$ for this class of materials, are characteristic of metamagnets with a critical field needed to induce the phase transition from a canted antiferromagnetic state at low fields to a new state with a larger magnetization at high fields. This new state, that corresponds to an inclination of spins towards the applied field direction, should be realized in the NMR experiments performed at high magnetic fields. Thus the antiparallel spin configuration observed by NMR should arise from the projection of the Mn^{III} spin along the field direction. The metamagnetic behavior implies that there is an anisotropy axis along a specific crystallographic direction, which is different from the applied field direction arising either from ligand field splitting or spin-orbit coupling. Since there is no direct exchange coupling between adjacent Mn spins, the resulting spin configuration can be attributed to quantum-mechanical²⁴ *antisymmetric spin-spin exchange* interactions. Antisymmetric interactions are based on a nonzero vector coefficient D , arising from the deviation²⁵ $\Delta g = g - 2$ of the mean value of the anisotropic gyromagnetic tensor g from its free-electron value of 2. Such a spin configuration is also consistent with the macroscopic ZFC thermomagnetic curves, indicating magnetic spin disorder.

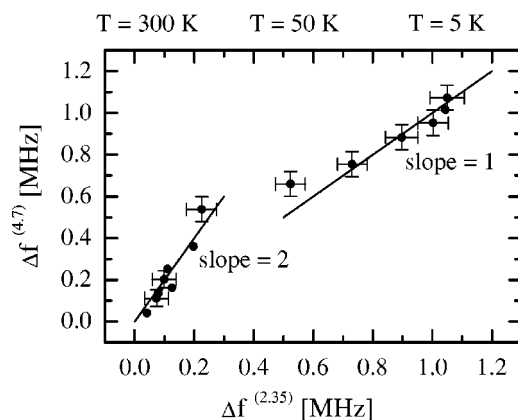


FIG. 8. $K^{(4.7)}$ vs $K^{(2.35)}$ with temperature as an implicit parameter. Selected temperatures to which the points are referred to, are indicated in the top axis. The solid lines indicate the two different slopes at high- and low-temperature regimes.

Another important feature of the observed NMR shifts is their field dependence. It is observed (Fig. 6) that at high temperatures down to about 80 K, $\Delta f^{(4.7)}$ is double $\Delta f^{(2.35)}$. This is what is expected for a paramagnetic state, i.e., the frequency shift to be proportional to the applied field. However, as the system is cooled down to 5 K, $\Delta f^{(4.7)}$ and $\Delta f^{(2.35)}$ gradually merge. This is quite unexpected for a shift of paramagnetic origin. This remarkable behavior is quantitatively demonstrated in Fig. 8, where $\Delta f^{(4.7)}$ and $\Delta f^{(2.35)}$ are plotted with temperature as an implicit parameter. The low- and high-temperature regimes are clearly indicated by the different slopes of the points. The solid lines in Fig. 8 have slopes equal to one and two and denote the low- and high-temperature regimes respectively. The fact that the absolute shift for each peak B and C is the same for the two different applied magnetic fields for temperatures below the transition temperature T_c , indicates clearly that this shift arises from a *spontaneous* hyperfine field at the proton site due to the frozen-in spin state of the system. Such NMR shifts that are independent of the applied field have been also observed in NMR studies of magnetic materials with ferromagnetic interactions in their ground states.^{26–28} Moreover, quite recently, extensive theoretical studies on ferrimagnetic chains, reveal the existence of such ferromagnetic interactions.^{29,30} In these works, it has been argued that the ground state of a ferrimagnetic chain may be recognized as a combination of ferromagnetic and antiferromagnetic features and is well explained in terms of the spin-wave theory.

In summary, the observed temperature dependence of the proton NMR shifts has revealed two magnetically nonequivalent Mn sites through the isotropic hyperfine coupling mechanism. These Mn sites reside in the planar rings of $[\text{MnTFPP}][\text{TCNE}]$. Also, it has been demonstrated that the hyperfine shifts are independent of the applied field in the magnetic-field range 2–5 T, indicating the presence of ferromagnetic interactions in the ground state of the molecular ferrimagnet, in accordance with theoretical works. To the best of our knowledge these experimental results are the first that provide microscopic information about the magnetic

configuration in this class of molecule-based magnets. The complexity of the magnetic structure of this material makes the identification of the spin configuration a difficult task, even for neutron-diffraction experiments. The NMR observation for antiparallel spin alignment provides substantial information for searching extra magnetic peaks in a neutron-diffraction pattern below T_c .

ACKNOWLEDGMENTS

We wish to acknowledge the following grants for support: The U.S. Department of Energy, Basic Energy Sciences Grants Nos. DE FG 02-86BR45271 and DE FG 03-93ER45504, and U.S. National Science Foundation Grant No. CHE-9730984.

*Email address: mfardis@ims.demokritos.gr

¹S. Chittipeddi, K.R. Cromack, J.S. Miller, and A.J. Epstein, *Phys. Rev. Lett.* **58**, 2695 (1987).

²O. Kahn, Y. Pei, M. Verdaguer, J.P. Renard, and J. Sletten, *J. Am. Chem. Soc.* **110**, 782 (1988).

³J.S. Miller, *Inorg. Chem.* **39**, 4392 (2000).

⁴K. Masinger, U. Schollwöck, S. Brehmer, H.J. Mikeska, and S. Yamamoto, *Phys. Rev. B* **58**, R5908 (1998).

⁵S. Yamamoto and T. Sakai, *Phys. Rev. B* **62**, 3795 (2000).

⁶J. Seiden, *J. Phys. (France) Lett.* **44**, L947 (1983).

⁷J.S. Miller and A.J. Epstein, *Chem. Commun. (Cambridge)* **1998**, 1319 (1998); W. Hibbs, D.K. Rittenberg, K. Sugiura, B.M. Burkhart, B.G. Morin, A.M. Arif, L. Liable-Sands, A.L. Rheingold, M. Sundaralingam, A.J. Epstein, and J.S. Miller, *Inorg. Chem.* **40**, 1915 (2001), and references therein.

⁸D.K. Rittenberg and J.S. Miller, *Inorg. Chem.* **38**, 4838 (1999); D.K. Rittenberg, A. Arif, and J.S. Miller, *J. Chem. Soc. Dalton Trans.* **2000**, 3939 (2000).

⁹D.K. Rittenberg, K. Sugiura, Y. Sakata, S. Mikami, A.J. Epstein, and J.S. Miller, *Adv. Mater.* **12**, 126 (2000).

¹⁰E.J. Brandon, A.M. Arif, B.M. Burkhart, and J.S. Miller, *Inorg. Chem.* **37**, 2792 (1998).

¹¹P. Zhou, B.G. Morin, A.J. Epstein, R.S. Mclean, and J.S. Miller, *J. Appl. Phys.* **73**, 6569 (1993).

¹²W.B. Brinckerhoff, B.G. Morin, E.J. Brandon, J.S. Miller, and A.J. Epstein, *J. Appl. Phys.* **79**, 6147 (1996).

¹³M.A. Girtu, C.M. Wynn, K.I. Sugiura, J.S. Miller, and A.J. Epstein, *J. Appl. Phys.* **81**, 4410 (1997).

¹⁴M. Balanda, K. Falk, K. Griesar, Z. Tomkowicz, and W. Haase, *J. Magn. Magn. Mater.* **205**, 14 (1999).

¹⁵C.M. Soukoulis and G.S. Grest, *J. Appl. Phys.* **55**, 1661 (1984).

¹⁶E. A. Turov and M. P. Petrov, *Nuclear Magnetic Resonance in Ferro- and Antiferromagnets* (Wiley, New York, 1972).

¹⁷The labeling of the proton sites is in accord with similar manganese porphyrin compounds (e.g. Ref. 10) where the structure has been determined.

¹⁸S.K. Mun, K. Mallick, S. Mishra, J.C. Chang, and T.P. Das, *J. Am. Chem. Soc.* **103**, 5024 (1981).

¹⁹G.N. La Mar and F.A. Walker, *J. Am. Chem. Soc.* **97**, 5103 (1975).

²⁰P. Turner and M.J. Gunter, *Inorg. Chem.* **33**, 1406 (1994).

²¹A.M. Clogston and V. Jaccarino, *Phys. Rev.* **121**, 1357 (1961).

²²The susceptibility data were obtained by normalizing our magnetization data at 4.7 T measured in arbitrary units with the susceptibility at low fields and at room temperature published in the literature (Ref. 8).

²³C.M. Wynn, M. Girtu, W.B. Brinckerhoff, K.I. Sugiura, J.S. Miller, and A.J. Epstein, *Chem. Mater.* **9**, 2156 (1997).

²⁴J. Krzystek, J. Tesler, L.A. Pardi, D.P. Goldberg, B.M. Hoffman, and L.-C. Brunel, *Inorg. Chem.* **38**, 6121 (1999).

²⁵F. Kefer, *Phys. Rev.* **126**, 896 (1962).

²⁶Y. Deligiannakis, G. Papavassiliou, M. Fardis, G. Diamantopoulos, F. Milia, C. Christides, K.I. Pokhodnia, and V. Barchuk, *Phys. Rev. Lett.* **83**, 1435 (1999).

²⁷Y. Furukawa, K. Watanabe, K. Kumagai, Z.H. Jang, A. Lascialfari, F. Borsa, and D. Gatteschi, *Phys. Rev. B* **62**, 14 246 (2000).

²⁸N.M. Wolcott, R.L. Falge, Jr., L.H. Bennett, and R.E. Watson, *Phys. Rev. Lett.* **21**, 546 (1968).

²⁹G.-S. Tian, *Phys. Rev. B* **56**, 5355 (1997).

³⁰S. Yamamoto, T. Fukui, and T. Sakai, *Eur. Phys. J. B* **15**, 211 (2000).